DOI: 10.18698/1812-3368-2018-5-45-53

INDUCTION OF A STRONG PARAMAGNETIC FIELD INSIDE PARTIALLY IONIZED AND WEAKLY MAGNETIZED PLASMA BY THE *E*×*B* DRIFT

D. Twaróg[1] dariusz.twarog@onet.pl
S.V. Ryzhkov[2] svryzhkov@bmstu.ru

[1] **Institute of Nuclear Physics, Kraków, Poland**
[2] **Bauman Moscow State Technical University, Moscow, Russian Federation**

Abstract

Partially ionized and weakly magnetized plasma compounded from natural gas and potassium seed flows along the outer cylindrical chamber, and is placed around the inner chamber. Inside the outer chamber, the azimuthal $E \times B$ drift induces a paramagnetic field B_p, with an intensity of tens of Teslas. The intensity of the B_p field is controlled by the inwardly directed radial electric field E and plasma temperature. The intensity of this field can be easily controlled by changes in the electric field E_{in}, produced by two co-axial placed cylindrical electrodes. Inside the inner chamber, the B_p field becomes antiparallel to the external magnetic field B_z. The theoretically obtained values of magnetic field in the outer chamber attains $B_p \sim 20.3$ T, and declines to ~ 13.5 T in the inner chamber

Keywords

Alternative system, magnetic field, plasma accelerator

Received 28.11.2017

Introduction. One of the major technical concerns in current fusion experiments is the energetic balance of the entire device. The most obvious way in which the energetic balance can be greatly improved is by using superconducting coils to produce a magnetic confinement field. This method was first introduced in the T-7 tokamak [1]. Superconducting coils has been widely used all over the world in projects such as Tore Supra (currently WEST), EAST, SST-1, KSTAR, and in new designs such as ITER [2]. However, despite having been used in such a wide array of projects, superconducting magnets still remain a source of serious technical problems. Moreover, in the future, they will be exposed to a much more intense neutron flux than in current experiments [3, 4].

This paper discusses the novel theoretical concept of generating magnetic fields, which is absolutely immune to heat and neutron fluxes from fusion plasma. According to the theoretical calculations the paramagnetic field (B_p) with intensities of tens of Teslas can be generated inside partially ionized and weakly magnetized plasma "mantle", which is continuously pumped along the outer chamber (z-axis direction). The intensity of this field is controlled and driven by the azimuthal electric drift $E \times B$, where B is self-sustained magnetic field. In the outer chamber, filled with a rotating plasma, the magnetic field: $B = B_z + B_p$ is the sum of the B_p field (induced by the $E \times B$ drift) and the external magnetic field $B_z = 2$ T. In the inner chamber, the B_p

field becomes anti-parallel to the B_z field. As a result, the magnetic field along the z-axis is expressed as follows: $B = B_p - B_z$.

Results of theoretical calculations obtained for unchanged density: $n(r) = 10^{25}$ m^{-3}, predicts, that during the paramagnetic field induction, plasma temperature rises from $T(r) \approx 0.47$ eV (injection position) to $T(r) \approx 0.85$ eV (exhaust position). This plasma, compounded mostly from natural gas and a potassium seed under the influence of the strong electric fields: $E \cong 4 \cdot 10^5$ V/m, the intensity of the paramagnetic field attains $B_p \sim 20.3$ T (inside the inner chamber). Magnetic field of such high intensity allows to confine and provide $D - {}^3\mathrm{He}$ plasma fusion [5, 6].

Plasma fluid equations. Proposed device is presented in Fig. 1, this is a simple cylindrical construction contained from two coaxially placed cylinders of the same length $l_c = 2$ m. Radius of the inner cylinder is $r_1 = 2$ m, radius of the outer cylinder is $r_2 = 2.5$ m. The device is equipped with two cylindrical electrodes placed on inner and outer cylinder, their task is to "maintained" the inwardly directed electric field: E_{in}. External magnetic coils provide the axial magnetic field $B_z = 2$ T. Between electrodes (inside the outer chamber) the magnetic field B is the sum of two parallel fields: the B_z field and the paramagnetic field B_p. However, inside the inner chamber according to the Maxwell law ($\nabla \cdot B = 0$) the B_p field become anti-parallel to the external magnetic field B_z. As is seen in Fig. 1, the proposed device is a combination of a typical MHD generator and a magnetic "trap" with a rotating plasma (a type "A" system according to the designation in Ref. [7]).

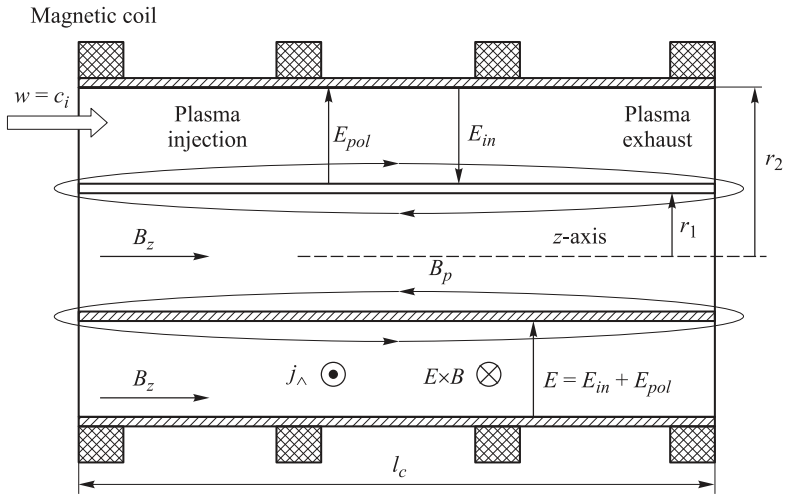

Fig. 1. Schematic view of proposed device with indicated electrodes, magnetic coils and plasma flow (external magnetic field, $B_z = 2$ T, minor radius of the outer chamber $r_1 = 2$ m, major radius $r_2 = 2.5$ m and length $l_c = 2$)

The treatment describes a dense quasineutral plasma rotating in a strong magnetic field, where $n_i \cong n_e = n_\alpha$. The mass m_N of a neutral particle is comparable to m_i. As a result, the theoretical description of the plasma flow in the study system is a combina-

tion of the treatment taken from Ref. [7, 8] and the typical MHD equations [9]. Adopting three-fluid formalism, the governing equations are the toroidal momentum equation for ions

$$n_i m_i \frac{\partial \mathrm{v}_{i\wedge}}{\partial t} = j_{i\perp} \times B - \nabla p_i + n_i m_i \eta_i (\nabla^2 \mathrm{v}_{i\wedge}); \\ -n_N n_i m_i \xi_N (\mathrm{v}_{i\wedge} - \mathrm{v}_{N\wedge}) + \frac{n_i m_i \mathrm{v}_{i\wedge}^2}{r}, \tag{1}$$

the toroidal momentum equation for electrons

$$n_e m_e \frac{\partial \mathrm{v}_{e\wedge}}{\partial t} = j_{e\perp} \times B - \nabla p_e - \frac{n_e m_e \mathrm{v}_{e\wedge}}{\tau_{eN}}, \tag{2}$$

the toroidal momentum equation for neutrals

$$n_N m_N \frac{\partial \mathrm{v}_{N\wedge}}{\partial t} = -\nabla p_N + n_N n_i m_N \xi_\mathrm{N} (\mathrm{v}_{i\wedge} - \mathrm{v}_{N\wedge}) - \frac{n_N m_N \mathrm{v}_{N\wedge}^2}{r}, \tag{3}$$

the conservation of particles

$$\frac{\partial n_\alpha}{\partial t} + \nabla \cdot (n_\alpha \mathrm{v}_{\alpha\wedge}) = -\frac{\partial n_N}{\partial t} - \nabla \cdot (n_N \mathrm{v}_{N\wedge}), \tag{4}$$

the current continuity equation

$$\nabla \cdot j = 0. \tag{5}$$

Here $\alpha = e, i$ denotes either ions or electrons, $\xi_N = \nu_{iN} / n_N$, and $\nu_{eN} = \mathrm{v}_e n_N \sigma_{eN}$ and $\nu_{iN} = \mathrm{v}_i n_N \sigma_{cx}$ are the electron-neutral elastic collisions and ion-neutral charge exchange collisions frequencies, respectively. Thermal velocities of electron and ion are given by v_e and v_i. In above model, the $\mathrm{v}_{N\wedge}$ represent neutral atoms velocity in the azimuthal direction, and η_i is the viscosity due to ion-ion collisions [10]. Currents: $j_{e\perp} = \sigma_{e\perp} E$ and $j_{i\perp} = \sigma_{i\perp} E$ (where: $\sigma_{\alpha\perp} = \sigma_{\alpha II} / (1 + x_\alpha^2)$) are flowing in radial direction.

Under influence of the axial magnetic field B and the radial electric field E, both electrons and ions started to rotate in the same azimuthal direction (Fig. 1). Within the study range of plasma parameters the ion viscosity and the centrifugal terms can be neglected, and one recovers the following formula for ion azimuthal velocity:

$$\mathrm{v}_{i\wedge} = \frac{j_{i\perp} \times B - \nabla p_i + n_i m_i \nu_{iN} \mathrm{v}_{N\wedge}}{n_i m_i \nu_{iN}}, \tag{6}$$

and for electrons

$$\mathrm{v}_{e\wedge} = \frac{j_{e\perp} \times B - \nabla p_e}{n_e m_e \nu_{eN}}. \tag{7}$$

Under assumptions that during the $E \times B$ drift neutrals remains in rest: $\mathrm{v}_{N\wedge} = 0$, Eqs. (6) and (7) can be simplify into one the classic formula:

$$\mathrm{v}_{\alpha\wedge} = \frac{E/B}{1+\left(\mathrm{v}_{\alpha N}^2/\omega_\alpha^2\right)} = \frac{\sigma_{\alpha II} x_\alpha E}{e n_\alpha \left(1+x_\alpha^2\right)}, \tag{8}$$

where: $x_\alpha = \omega_\alpha / \mathrm{v}_{\alpha N}$, $\omega_{\alpha c} = eB/m_\alpha$, $\sigma_{\alpha II} = e^2 n_\alpha / \left(\mu_{\alpha N}\mathrm{v}_{\alpha N}\right)$ is the scalar electron or ion electrical conductivity, $\mu_{\alpha N}$ is the reduced mass [11–13].

Inside outer chamber under the $E\times B$ drift influence electrons and ions starting to rotate into the same azimuthal direction. However, collisions with the neutral gas cause the electrons and ions to have different azimuthal velocities. In a partially ionized $\mathrm{v}_{ei} > \mathrm{v}_{eN}$ and weakly magnetized plasma $x_e = \omega_{ec}/\mathrm{v}_{eN} \gg 1$ and $x_i = \omega_{ic}/\mathrm{v}_{iN} \approx 1$. The ion-neutral collisions reduce the ion azimuthal velocity $\mathrm{v}_{i\wedge}$ to a value lower than the electron azimuthal velocity $\mathrm{v}_{e\wedge}$. The difference between them gives the Hall current:

$$j_\wedge = n_\alpha e\left(\mathrm{v}_{e\wedge} - \mathrm{v}_{i\wedge}\right) = \left(\sigma_{e\wedge} - \sigma_{i\wedge}\right) E. \tag{9}$$

Within the study range of plasma parameters the friction force acting on neutrals is much more higher than viscosity, in result, neutral atoms starts to rotate with ions: $\mathrm{v}_{N\wedge} \neq 0$. According to eq. (3) the azimuthal neutral velocity can be expressed as follows:

$$\mathrm{v}_{N\wedge} = \frac{-\nabla p_N + n_i m_N \mathrm{v}_{iN}\mathrm{v}_{i\wedge}}{\left(n_N m_N + n_i m_N \mathrm{v}_{iN}\right)}. \tag{10}$$

Inserting of eq. (10) into (6) allows to estimate the ion azimuthal velocity:

$$\mathrm{v}_{i\wedge} = \frac{j_{i\perp}\times B - \nabla p_i - \dfrac{\nabla p_N n_i m_i \mathrm{v}_{iN}}{m_N\left(n_N + n_i \mathrm{v}_{iN}\right)}}{n_i m_i\left(1 + \mathrm{v}_{iN} - \dfrac{n_i m_N \mathrm{v}_{iN}^2}{m_N\left(n_N + n_i \mathrm{v}_{iN}\right)}\right)}. \tag{11}$$

Equations (7), (9) and (11) allow to correctly calculating intensity of the Hall current for: $\mathrm{v}_{N\wedge} \neq 0$, and will be using in all further calculations. It is worth to mention that plasma injection under "acute" angle to the *z*-axis opens a possibility to create the azimuthal component anti-parallel to the $\mathrm{v}_{N\wedge}$ velocity (gained as a result of collisions). However this case will not be study further in this paper.

Paramagnetic field induction. In presented concept plasma is obtained by burning the natural gas (mostly methane CH_4 ~ 97 % and ethane C_2H_6 ~ 3 %) in oxygen enriched air (~ 45 % of volume), combustion takes place outside the study area. In result, plasma temperature attains ~ 2300 K [14], and with the help of external sources is further raised up to the required injection temperature: ~ 0.47 eV. Another step is to add a seed (alkaline metal) to provide the necessary number of free electrons required for an adequate electrical conductivity [15]. It has been found that by adding a small amount of a seed — in the range of 0.01…1.0 % by volume — the threshold ionization temperature is reduced by as much as 60…70 % [16]. In the case study, different ratios of seed (potassium K) to full gas weight (%) were studied in the aim to select compositions of the best parameters. Such prepared plasma (CH_4/K) of density $n(r) \sim 10^{25}\,\mathrm{m}^{-3}$ and temperature 0.47 eV is injecting between electrodes, under the

$E \times B$ drift influence electrons and ions starting to rotate into the same azimuthal direction but with different velocities. This difference gives the Hall current $j_\wedge$.

The paramagnetic field B_p is induced by the azimuthal current: $j_\Phi \cong j_\wedge + j_F - j_d$, where j_d is the plasma diamagnetic current and $j_F = n_\alpha (F_H - F_R) \times B / B^2$ is plasma current driven by radial acceleration dependent from the difference between the Hoop force: $F_H = j_\wedge \times (B_p + B_z)/n_\alpha$ [17], and the friction force in radial direction: $F_R = n_i m_N \xi_N (\mathrm{v}_{ir} - \mathrm{v}_{Nr})$. Within the study range of parameters $j_\wedge \gg j_d$ and $j_\wedge \gg j_F$ what makes that intensity of the paramagnetic field is only controlled and proportional to the Hall current intensity. Remember that $j_\wedge = (\sigma_{e\wedge} - \sigma_{i\wedge})E$ and $\sigma_{\alpha\wedge} = \sigma_{\alpha II} x_\alpha \big/ \left(1 + x_\alpha^2\right)$ is easy to see that the intensity of the paramagnetic field attainable under certain plasma density, temperature and electric field is restrained by the magnetic field itself: $B_p \sim 1/B$. Distributions of the paramagnetic fields (B_p) were calculated using (see Ref. [18]). Graphic solutions obtained for: $\mathrm{v}_{N\wedge} \neq 0$, different temperatures and chemical compositions are presented in Fig. 2. In an effort to simplify calculations, the following assumptions were used:

(i) equals ion, electron and neutrals temperatures $T_e = T_i = T_N = T(r)$;

(ii) plasma density is given by $n(r) = n_0 \exp\left[-(r-\mu)^2 / 2\sigma^2\right]$;

(iii) initial plasma temperature is given by $T(r) = T_0 \exp\left[-(r-\mu)^2 / 2\sigma^2\right]$.

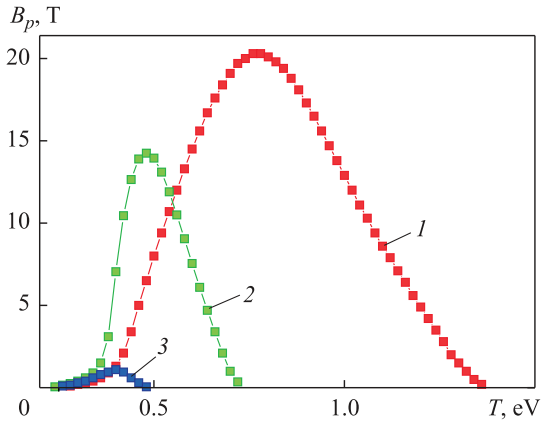

Fig. 2. Distributions of the paramagnetic fields for different plasma temperatures and compositions obtained at $r = 2.25$ m, $l_c = 2$ m, $n_0 = 10^{25}$ m^{-3}, $B_z = 2$ T and $E = 4 \cdot 10^5$ V/m:
1 — $K = 1$ %; *2* — $K = 10$ %; *3* — $K = 20$ %

The density and temperature distributions were obtained for: $n_0 = 10^{25}\,\mathrm{m}^{-3}$, $T_0 = 0.47$ eV and $\sigma = 0.5$, $\mu = 2.25$. For the needs of calculations methane cross-section and potassium was taken from Ref. [19].

As is seen in Fig. 2 intensity of the paramagnetic field is strongly dependent on plasma temperature $T(r)$, density $n(r)$ and chemical composition. The B_p field intensity is also proportional to the azimuthal cross-section of the plasma "mantle": $s_\perp = l_c d$ (where $d = r_2 - r_1 = 0.5$ m) and the electric field intensity (E), which have to

be inwardly directed: $E_{in} > E_{pol}$ and intense enough to give: $j_\wedge > j_d$ [18]. Plasma containing higher abundances of potassium is not convenient for the paramagnetic field induction, because intensity of the B_p field declines sharply with increase of potassium concentration (Fig. 2). Optimum composition seems to be a plasma containing from potassium (1 %) and CH_4 (99 %), for that composition significant part of the "background" temperature (~ 0.2 eV) came from chemical burning. For that plasma, intensity of the B_p field attains ~20.3 T at ~ 0.77 eV (curve *1* in Fig. 2). Raising concentration of potassium, result in shifting a maximum of the paramagnetic field into the low temperatures area, at 10 % potassium concentration, the B_p field attains maximum ~ 14.25 T at ~ 0.48 eV (curve *2* in Fig. 2). Further increase of potassium concentration provide to sharply declines intensity of the paramagnetic field, for plasma containing 20 % of potassium (curve *3* in Fig. 2) the B_p field attains ~ 1.1 T at ~ 0.4 eV. In all study cases intensity of the paramagnetic field starts to rise rapidly together with the temperature growth. Temperature rise provide a new dose of ions and electrons but when the ionization degree exceed certain level: $\alpha_K \approx 0.5$ (for potassium) in other words, when there are not enough neutrals to impose a significant drag force on charged particles the paramagnetic field stop to rise. Declining numbers of neutrals in response to increased temperature causes an "exponential" drop in the intensity of the paramagnetic field. Detailed analysis (see Ref. [18]) revel that the fastest rises of the paramagnetic field intensity is notice in the relatively weak electric fields: $E < 10^4$ V/m, the grooving rate becomes weaker in stronger electric fields: $E > 10^5$ V/m. This is why ions become magnetized ($x_i \sim B$) in stronger magnetic fields. As a result, the ion conductivity ($\sigma_{i\wedge}$) rises, which reduces the Hall current: $j_\wedge = (\sigma_{e\wedge} - \sigma_{i\wedge})E$. This mechanism, together with heating, limits the paramagnetic field B_p values for a given radial electric field: $E = E_{in} + E_{pol}$.

Radial electric field. The radial electric field (E) is the sum of two electric fields: the inwardly directed field (E_{in}); and the polarization electric field (E_{pol}). The inwardly directed field $E_{in} = 4 \cdot 10^5$ V/m is produced by two cylindrical electrodes placed on the inner and outer walls (Fig. 1). The inwardly directed electric field induces a parallel flowing current: $j_\perp = (\sigma_{e\perp} + \sigma_{i\perp})E_{in}$ (where $\sigma_{\alpha\perp} = \sigma_{\alpha II} / (1 + x_\alpha^2)$), which drags charged particles of different signs in opposite directions [20]. In the geometry presented, this results in a space charge imbalance, ρ_e, which is expressed as:

$$\rho_e = -\varepsilon_0 \frac{E^*}{\sigma_{eII}} \nabla\sigma_{eII} - \varepsilon_0 B(\nabla \times w) - \varepsilon_0 \left(\frac{\omega_{ec}\tau_{eN}}{\sigma_{eII} B} j_e - w \right)(\nabla \times B) +$$

$$+ \varepsilon_0 \frac{\omega_{ec}\tau_{eN}}{\sigma_{eII} B} B(\nabla \times j_e) + \frac{\varepsilon_0 (j_e \times B)\nabla T^{1/2}}{e n_e T^{1/2}}, \qquad (12)$$

where $E^* = E_{in} + w \times B$, $\tau_{eN} = \nu_{eN}^{-1}$ [21].

In the presented device, plasma is injected with the ion sound velocity $w \approx c_i = \sqrt{kT(r)/m_i}$, parallel to the magnetic field, as a result: $w \times B = 0$ what gives:

$E^* = E_{in}$. The result obtained with the help of (12) enabled calculation of the polarization field (E_{pol}) and the field distribution ($E = E_{in} + E_{pol}$). For the case presented in Fig. 3, it was done for the same set of plasma parameters as the paramagnetic fields presented in Fig. 2. The charged-particles imbalance needed to establish a radial electric field with an intensity of $E \cong 3.7 \cdot 10^5$ V/m at $r \approx 2.25$ m is small: $\Delta n_e / n_e \sim 10^{-10}$. This imbalance does not disrupt the quasi-neutrality of the plasma. According to (12), the intensity of the polarization electric field depends on plasma parameters such as density $n(r)$ and temperature $T(r)$, but it can also be controlled by changes of intensity in the E_{in} field and gradient of scalar conductivity $\nabla\sigma_{e\text{II}}$. Within the range of study plasma parameters, above approximation gives the E_{pol} field of top intensity ($\approx 7.5 \cdot 10^4$ V/m) lower than the E_{in} field ($4 \cdot 10^5$ V/m). As a result, the E field is directed inwardly and can induce the paramagnetic field.

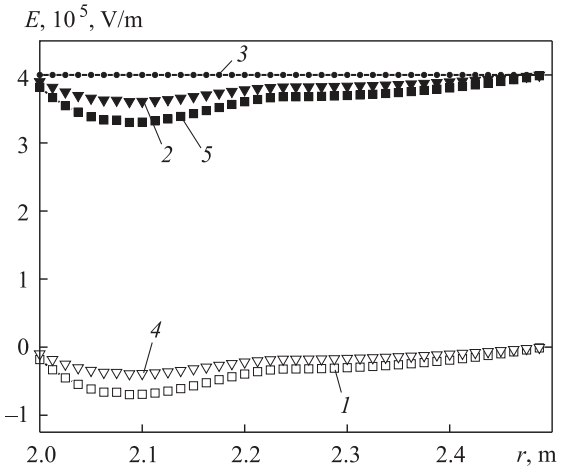

Fig. 3. Electric field distributions between inner and outer electrode obtained for heating effects in exhaust position (*1* — E_{pol}, *5* — $E = E_{in} + E_{pol}$, T = 0.47 eV) and without heating effects close to injection position (*4* — E_{pol}, *2* — $E = E_{in} + E_{pol}$, T = 0.85 eV); temperature and paramagnetic field B_p distributions are taken from Fig. 2; *3* — E_{in}

Conclusions. The paramagnetic field B_p is driven and controlled by the azimuthal $E \times B$ drift, which induces the azimuthal current. Potassium injection result in an increase of Hall current intensity ($j_\wedge \sim B_p$), because the Hall current intensity, $j_\wedge = n_\alpha e(\mathrm{v}_{e\wedge} - \mathrm{v}_{i\wedge})$, rises together with ion mass (electrons still rotate with the same azimuthal velocity $\mathrm{v}_{e\wedge}$ as opposed to heavier ions, $\mathrm{v}_{i\wedge} \sim T^{3/4} / m_i^{3/2}$). It is seems that among from the study plasma mixtures (CH_4/K), composition contained of CH_4 (99 %) and potassium (1 %) seems to be the most convenient option. High intensity of the B_p field (~ 20.3 T) can be attained under relatively low temperature (~ 0.77 eV) and relatively low potassium abundances. The theoretically obtained values of magnetic field require the experimental confirmation, e.g. on such device as CTC [22–24]. However, results preneted in Section II and theoretical discription

given by eqs. (1)–(5), (10) and (11) shown that the $E \times B$ drift can induce the magnetic field of high intensity in partially ionised plasma contained from at least two specious of significantly different ionisation energy. Within the temperature frame, when one of that component is ionised and the second still remain neutral.

Values of the paramagnetic field discussed in this paper are close to those of the initial magnetic field required in the MagLIF project (10…50 T). In this project, an axial magnetic field is amplified by a factor of 10^2–10^3 within the fuel-filled volume of the imploding liner via magnetic flux compression [25]. If we took into account plasma volume, proposed concept is more similar to the LINUS project [26] and to their continuation provided by General Fusion [27].

Taking into account thermal resistance and radiation resistance, the above approach to magnetic field production can be considered an alternative to the "classical" conductors, and even to the superconducting coils, especially if we take into account the complexity of the entire construction (cryostat, neutron shielding).

REFERENCES

[1] Ivanov D., Keilin V., Stavissky B., Chernoplekov N. Some results from the T-7 Tokamak superconducting magnet test program. *IEEE Trans. on Mag.*, 1979, vol. 15, iss. 1, pp. 550–553. DOI: 10.1109/TMAG.1979.1060275

[2] Sharma R.G. Superconductivity. Basics and applications to magnets. Springer, 2015. Pp. 305–357.

[3] Ulbricht A., Duchateau J.L., Fietz W.H., Ciazynski D., et al. The ITER toroidal field model coil project. *Fusion Eng. Des.*, 2005, vol. 73, iss. 2-4, pp. 189–327. DOI: 10.1016/j.fusengdes.2005.07.002

[4] Gilbert M.R., Dudarev S.L., Zheng S., Packer L.W., Sublet J.-Ch. An integrated model for materials in a fusion power plant: transmutation, gas production, and helium embrittlement under neutron irradiation. *Nuclear Fusion*, 2012, vol. 52, no. 8, art. 083019. DOI: 10.1088/0029-5515/52/8/083019

[5] Ryzhkov S.V. Comparison of a deuterium-elium-3 FRC and mirror trap. *Fusion Science and Technology*, 2007, vol. 51, iss. 2T, pp. 190–192. DOI: 10.13182/FST07-A1347

[6] Ryzhkov S.V. Compact toroid and advanced fuel — together to the Moon?! *Fusion Science and Technology*, 2005, vol. 47, iss. 1T, pp. 342–344. DOI: 10.13182/FST05-A684

[7] Lehnert B. Rotating plasmas. *Nuclear Fusion*, 1971, vol. 11, no. 5, pp. 485–533. DOI: 10.1088/0029-5515/11/5/010

[8] Lehnert B. Screening of a high-density plasma from neutral gas penetration. *Nuclear Fusion*, 1968, vol. 73, no. 8, pp. 173–181. DOI: 10.1088/0029-5515/8/3/005

[9] Galeev A.A., Sudan R.N., eds. Basic plasma physics. Selected chapters. Elsevier, 1989. 32 p.

[10] Braginskii S.I. In Reviews of plasma physics. Vol. 1. Consultants Bureau, 1965. 205 p.

[11] Rozhansky V.A., Tsendin L.D. Transport phenomena in partially ionized plasma. Taylor and Francis, 2001. 488 p.

[12] Fridman A., Kennedy L.A. Plasma physics and engineering. CRC Press, 2011. 941 p.

[13] Danielsson L. Review of the critical velocity of gas-plasma interaction. *Astrophysics and Space Science*, 1973, vol. 24, iss. 2, pp. 459–485. DOI: 10.1007/BF02637168

[14] Chernyshev V. International co-operation in MHD electrical power generation. *IAEA Bulletin*, 1977, vol. 20, no. 1, pp. 42–53.

[15] Dhareppagol V.D., Saurav A. The future power generation with MHD generators magneto hydrodynamic generation. *IJAEEE*, 2013, vol. 2, no. 6, pp. 101–105.

[16] Louis J.F. Closed cycle magnetohydrodynamic generator. US Patent 3487240. Appl. 09.02.1966, publ. 30.12.1969.

[17] Wesson J. Tokamaks. Oxford, Clarendon, 1997. 694 p.

[18] Twaróg D. Field reversed configuration induced by a paramagnetic field. *IEEE Trans. Plasma Sci*., 2013, vol. 41, iss. 2, pp. 280–289. DOI: 10.1109/TPS.2013.2240019

[19] Song Mi-Y., Yoon J.-S., Cho H., Itikawa Y., Karwasz G.P., Kokoouline V., Nakamura Y., Tennyson J. Cross sections for electron collisions with methane. *J. Phys. Chem. Ref. Data*, 2015, vol. 44, iss. 2, pp. 2–20. DOI: 10.1063/1.4918630

[20] Chen F.F. Introduction to plasma physics and controlled fusion. Plenum Press, 1974. 329 p.

[21] Celiński Z.N. The effect of cold, electrode boundary layers on the electrical characteristics of DC MHD generators. *Nukleonika*, 1966, no. 11, pp. 615–628.

[22] Romadanov I.V., Ryzhkov S.V. Compact toroid challenge experiment with the increasing in the energy input into plasma and the level of trapped magnetic field. *Fusion Engineering and Design*, 2014, vol. 89, iss. 12, pp. 3005–3008. DOI: 10.1016/j.fusengdes.2014.09.001

[23] Romadanov I.V., Ryzhkov S.V. Regimes of pulsed formation of a compact plasma configuration with a high energy input. *Plasma Physics Reports*, 2015, vol. 41, iss. 10, pp. 814–819. DOI: 10.1134/S1063780X15100074

[24] Mozgovoy A.G., Romadanov I.V., Ryzhkov S.V. Formation of a compact toroid for enhanced efficiency. *Physics of Plasmas*, 2014, vol. 21, iss. 2, art. 022501. DOI: 10.1063/1.4863452

[25] Shipley G.A., Awe T.J., Hutsel B.T., Slutz S.A., Lamppa D.C., Greenly J.B., Hutchinson T.M. Megagauss-level magnetic field production in cm-scale auto-magnetizing helical liners pulsed to 500 kA in 125 ns. *Physics of Plasmas*, 2018, vol. 25, iss. 5, art. 052703. DOI: 10.1063/1.5028142

[26] Quimby D.C., Hoffman A.L., Vlases G.C. LINUS cycle calculations including plasma transport and resistive flux loss. *Nuclear Fusion*, 1981, vol. 21, no. 5, pp. 553–570. DOI: 10.1088/0029-5515/21/5/005

[27] General Fusion: company website. Available at: http://www.generalfusion.com (accessed: 05.09.2017).

Twaróg D. — Ph.D., Institute of Nuclear Physics (Radzikowskiego 152, Kraków, 31-342 Poland).

Ryzhkov S.V. — Dr. Sc. (Phys.-Math.), Professor, Department of Thermophysics, Bauman Moscow State Technical University (2-ya Baumanskaya ul. 5, str. 1, Moscow, 105005 Russian Federation).

Please cite this article as:

Twaróg D., Ryzhkov S.V. Induction of a Strong Paramagnetic Field Inside Partially Ionized and Weakly Magnetized Plasma by the *E*×*B* Drift. *Vestn. Mosk. Gos. Tekh. Univ. im. N.E. Baumana, Estestv. Nauki* [Herald of the Bauman Moscow State Tech. Univ., Nat. Sci.], 2018, no. 5, pp. 45–53. DOI: 10.18698/1812-3368-2018-5-45-53